Draft version May 12, 2023
Typeset using LaTeX default style in AASTeX631

Determining the Distance, Age, and Color Excess of NGC 2323

Thomas Tran[1]

[1]San Diego State University, 5500 Campanile Dr, San Diego, CA 92182

ABSTRACT

This manuscript was written to measure the distance, age, and color excess of star cluster NGC 2323. Stars within the coordinates RA 07h 02m 42s and Dec -08d 23m 00s were filtered through a process where we isolated the cluster stars from local background and foreground stars. Isochrone population data from the CMD web interface Rose (2018) was given to compare model predictions in order to measure the age and color excess of NGC 2323 through the chi-square minimization technique. We will run through the astronomical techniques used to calculate the parameters of our cluster, NGC 2323.

1. INTRODUCTION

When observing clusters in the night sky, astronomers are looking at stars from a wide range of distances. Clusters of stars move together and can pass by other stationary stars. There are methods used by astronomers to characterize star clusters, which we will explore through this paper. Before going through these methods, we will first talk about what star clusters are and where they come from. The initial mass of a star determines its lifespan, brightness, and how its color and brightness will change as it ages. Stars that are formed within the same cloud of gas are all around the same distance from us and all have similar proper motions. Using the proper motion of the cluster allows astronomers to separate stars from the cluster and the other stars in view. The color of stars can also tell us a great deal about their mass. Stars that are blue are much more massive than red stars. The more massive a star is, the brighter it appears in the sky. For example, the brightest star in our night sky, Sirius, is a massive blueish-white star. These massive blue stars have much shorter lifespans than less massive red stars because they burn through their fuel far quicker.

Measuring the distance to clusters can be difficult due to interstellar extinction. Extinction occurs when the light from stars pass through interstellar dust and appears redder to observers on Earth. This not only affects the color we see, but also the brightness of the star. The B-V color increases through extinction which explains the star's redder appearance. Astronomers can get around extinction by converting the observed reddening, also known as color excess, to a visual extinction along the line of sight to a target star. With the given constant of proportionality, R = 3.1, we know the ratio of total extinction compared to selective extinction. This ratio tells us how much the light is reddened and how much starlight is extinguished. We can find the value of R by looking at the internal extinction within a cluster. A large R value constitutes larger dust grains which in turn means higher extinction. Before the distance to a cluster is measured, we can determine the absolute magnitude and intrinsic color of stars through photometric observations. By taking the difference between observed and intrinsic B-V color measurements, we can obtain the color excess, E(B-V). The product of color excess ($E(B\text{-}V)$) and the ratio of extinction (R), results in the visual extinction.

$$m_V - M_V = 5log\left(\frac{d}{10}\right) + 3.1E(B-V) \tag{1}$$

$$E(B-V) = [(B-V)_{\rm obs} - (B-V)_{\rm int}] \tag{2}$$

Using the distance modulus in eqn. (1) above, M_V and $(B-V)_{\rm int}$ can be calculated from the observations of our star. With the observed values of m_V and $(B-V)_{\rm obs}$, we can measure the distance to the star.

The interstellar dust particles found in extinction are created from heavy elements within the atmosphere of red giants. Shorter wavelengths of light, such as the color blue, are scattered through the dust more than longer wavelengths of light. The dust changes the color ($B\text{-}V$) of the star. The color in the B-band is reduced, so the B-V of the observed

star will not match the intrinsic color of the star. Without considering the absorption, we would not be able to measure the absolute magnitude of the star and determine its distance. There are stellar population models that have been made to show the typical life cycle for different types of stars. In these models, we can see stars along the main sequence sorted by brightness and color at different times. We can apply our cluster data to these model predictions to measure the age of our cluster.

2. DATA

Images of NGC 2323 were captured with the one-meter telescope at Mount Laguna Observatory (MLO). There were a total of 25 bias images and 12 twilight flats. Half of the flats were in the B-band and the other half were in the V-band. Lastly, there were 6 images taken (3 for each filter) of the cluster with different exposure times. The exposure times were 5, 20, and up to 80 seconds. We take shorter exposures to record the magnitudes of the brighter stars, and longer exposures for the fainter stars.

The Gaia Collaboration et al. (2016) database was utilized to query our right ascension (RA) and declination (Dec) of all stars within the field of our cluster. We stored the identifier, distance, distance uncertainty, and proper motion in RA and Dec for the stars into a table in order to use for photometry. We then used the APASS catalog by Henden et al. (2016), in order to attain the B and V magnitude of the stars within our cluster. We used the stars from APASS as our reference stars when calculating the zeropoint magnitude for the images from MLO.

Lastly, we used the CMD web interface by Rose (2018) in order to access stellar population models. These models helped us determine the age and color excess of NGC 2323. The models contain expected B-band and V-band magnitudes for populations of stars at different ages ranging from tens of millions to billions of years old. We were given the ratio between total and selective extinction, $R_V = \frac{A_V}{E(B-V)} = 3.1$ and the B-band/V-band ratio, $\frac{A_B}{A_V} = 1.297$ for the conversion of observed magnitudes to absolute magnitudes.

3. ANALYSIS

The RAW B-band and V-band images of NGC 2323 were taken through an astronomical technique of processing. First, the overscan from the images were removed. Overscan from images are unexposed regions of each image taken at the same time as the collected data. After the overscan was subtracted from the image, we debiased the images. The process of debiasing involves subtracting our bias frames, which are special images taken with the telescope but with zero exposure time. The bias frame captures the inherent noise and electronic offset in the detector and is used to calibrate the images by removing these effects. Next, we took our flat field images and processed them into a master flat field to further correct the images. According to Starck et al. (2002), creating a master flat field calibration consists of removing spatial variations in the detector response. Flat fielding corrects for the sensitivity differences across the detector, caused by variations in the pixel-to-pixel response or dust on the optical surfaces. The process of creating a master flat field calibration involves taking a series of flat field images, which are images of a uniform light source that illuminates the entire detector. The flat field images are then combined to create a master flat field calibration image, which represents the average response of the detector to a uniform input. The master flat field calibration is then divided into each image, to correct for the detector response. Each of our images were processed through the removal of overscan, debiasing, and were corrected for flat-field effects.

In order to measure the brightness of the stars within our cluster, we first located each star within the field. We used the Gaia database Gaia Collaboration et al. (2016) to query for known stars within 8 arcmin of the cluster and have a G-band pass less than 19^{th} magnitude ($G_{\text{BP}} < 19$) with parallaxes that are at least 5 times greater than the uncertainty. The magnitude cutoff of $G_{BP} < 19$ mag ensures that we retrieve stars that are relatively bright and have high-quality photometry. This reduces the impact of photometric errors and uncertainties, which can be larger for fainter stars. The parallax criterion of at least 5 times greater than the uncertainty ensures that the retrieved stars have high-quality measurements. The queried stars were plotted in Figure (1) below.

We pulled our reference stars from the VizieR catalog (APASS) to get the B and V magnitudes of our stars. The data from this catalog was used to calculate the zeropoints for the images from MLO. The zeropoints are for our photometry measurements when converting counts into magnitudes. After matching the stars within our cluster from APASS to Gaia, we created a list of all of the matching stars. The closely matched stars can be seen in Figure (2) below. All of the stars were matched by their locations.

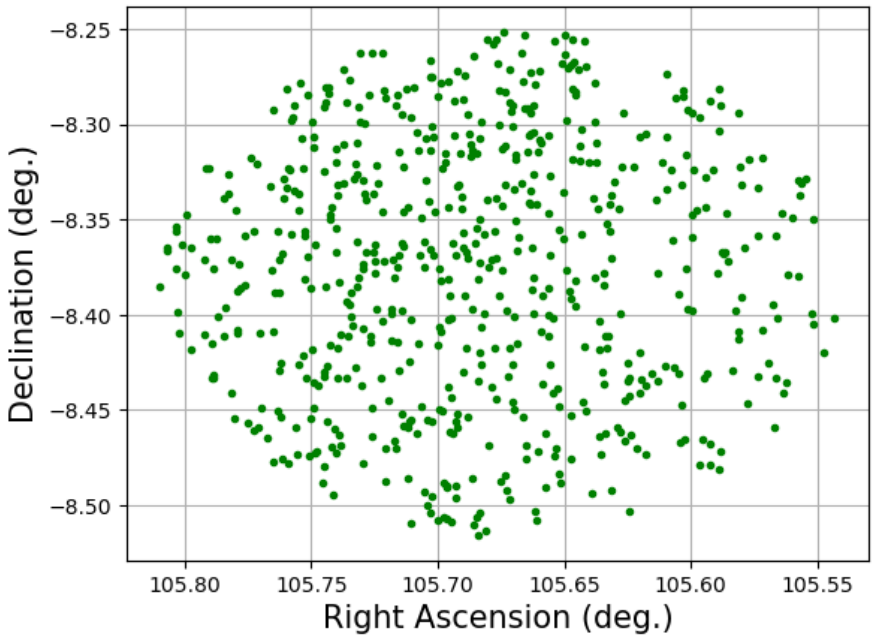

Figure 1. Shows the location of stars within our target field within 8 arcmin from the Gaia database.

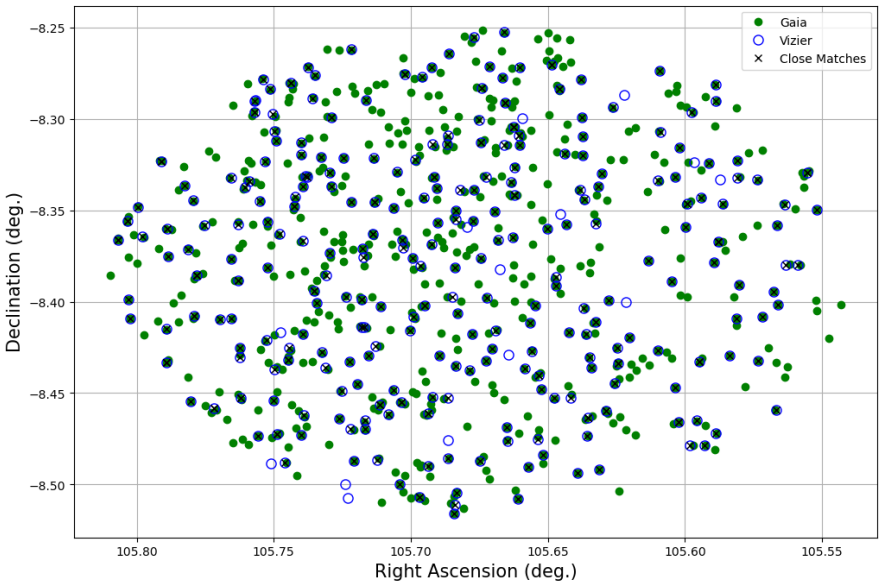

Figure 2. Similar to Figure (1), the location of stars within our target field are shown with close matches from the APASS catalog. The x marks signify stars that are most likely the same from both catalogs. The stars were matched if they were within 8 arcsec of each other.

After matching the stars from the two catalogs, we measured the B and V-band brightness of the matched stars, but from our MLO images. First, we needed to get the counts by taking the Analog-to-Digital Unit (ADU) counts and subtracting the background counts. A circular aperture of 1-full width half maximum were placed around the stars in the images to measure the counts from each source. If there were any stars that surpassed the linearity limit of 50,000 counts, they were considered oversaturated and were not recorded. The background counts were measured by getting the counts from a dark region in the image containing no stars. The background counts were subtracted from the total counts from the the circular aperture so that we could get an accurate count for each image.

Then, we took the number of counts and converted them into observed magnitudes. Using the magnitudes from the APASS catalog, we were able to get the zeropoint for each of the images. After computing the photometry, we were left with the observed mag. of the stars in our cluster. With the observed mag. from our photometry, we were able to generate a plot a color-magnitude diagram showing our cluster on the main sequence. The plot can be seen below in Figure (3).

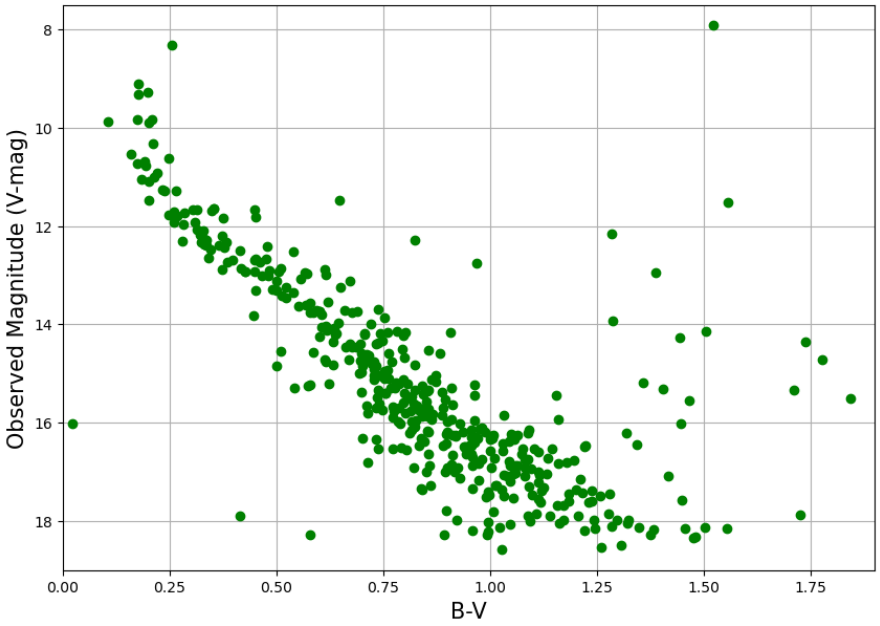

Figure 3. Shows a Color-Magnitude diagram of the stars within our field using magnitudes from our NGC 2323 data file. The main diagonal collection of stars running from top left to bottom right represent the main sequence.

One of the last steps was to determine which stars were actually in the cluster of NGC 2323. There are stars that reside in the foreground and background of the cluster and some are even at the same distance as the cluster. Thankfully we know that the stars in our cluster were formed together and have similar proper motions. Using our data, we were able to measure the distance to our cluster by plotting the histogram of Gaia distances to each star. The number of stars were greatest at about 1000 pc away. The histogram can be seen below in Figure (4).

We did the same thing with the proper motions, filtering out the stars with proper motions that were outside of the distribution. By filtering the stars by proper motion, we were able to separate stars that are actually in the cluster from the stars that just happen to be in the same part of the sky as NGC 2323. In order to generate an accurate color-magnitude diagram for our cluster, we needed to make sure we had good quality data for our B-V and magnitudes. We set a limit of 10 arc seconds for stars to be excluded if they were within this range because it is difficult to measure the light from two layered stars.

Through chi-square minimization, we measured the best age and color excess of NGC 2323. Along with stellar population models from the CMD web interface by Rose (2018), we plotted the cluster through different time sequences to estimate how old our cluster is. The plot with the different age models of our cluster can be seen below in Figure (5). The observed magnitudes were converted to absolute magnitudes before plotting on the color-magnitude plot. The models were shifted in distance and reddening to find the best fit for the cluster data and the chi-square value was calculated. To calculate the chi-square value, we compared the magnitudes and colors to the predicted properties of stars generated by the cluster model. Specifically, for each observed star, we calculate the difference between its observed value and the predicted value from the cluster model, and then square the difference. We do this for all observed stars in the sample, and sum up the squared differences to obtain the chi-square value. The lower the chi-squared value, the better our results are.

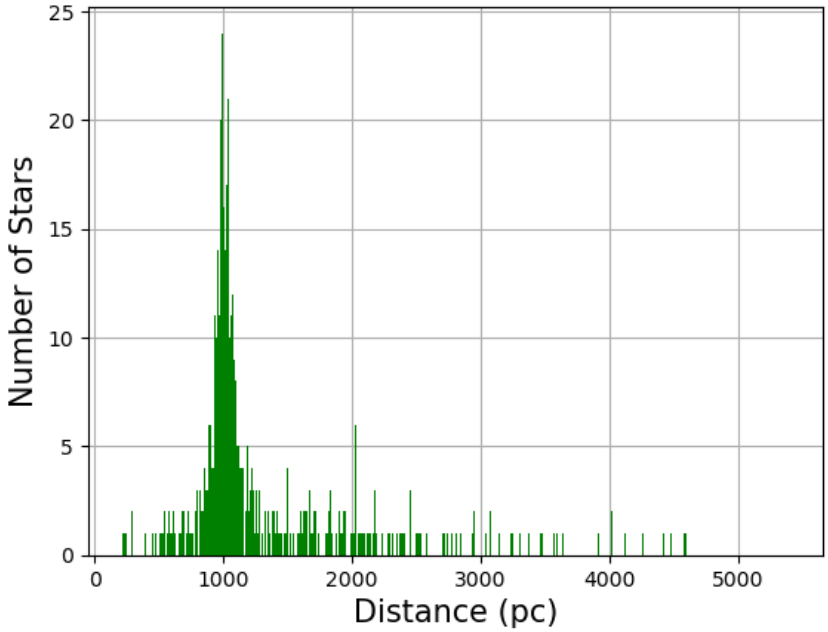

Figure 4. Histogram showing the highest number of stars at about 1000 parsecs away.

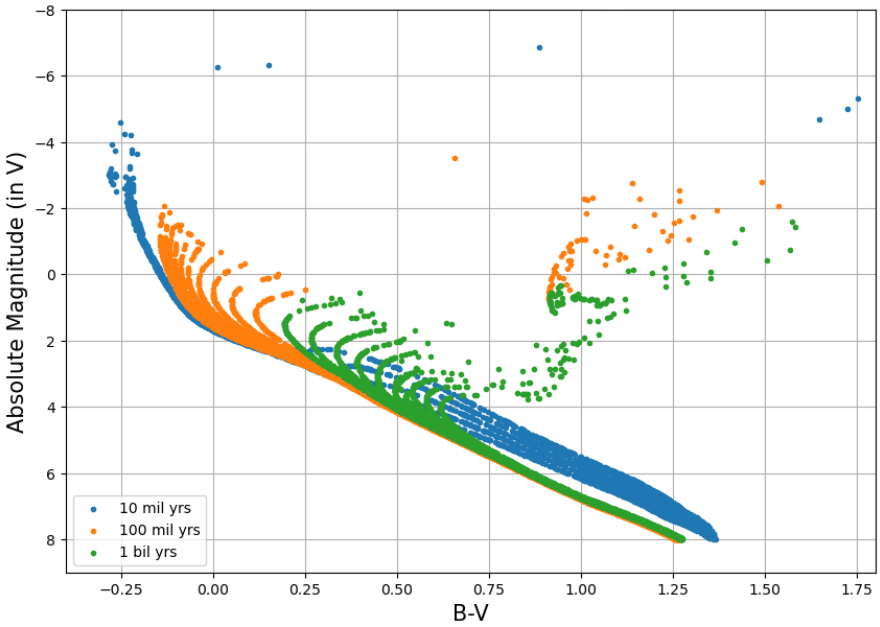

Figure 5. A collection of three different Color-Magnitude diagrams generated from the isochrone population data by Rose (2018). This figure displays the process of stellar evolution, each population shifts towards the right on the B-V scale as the color of the star changes over time. The oldest stars (in green) are shifted the furthest down and to the right meaning they have become dimmer and redder through billions of years.

4. DISCUSSION

Earlier when completing the first part of the project, we ran into issues with computing the photometry of the stars in our cluster. We were unable to obtain the observable magnitudes of the stars in NGC 2323, but fortunately we were given the data in the second part of the project. With the given data, we were able to measure the distance to our cluster and ultimately isolate the stars in NGC 2323 from any foreign stars in the same field. By setting a limit on the distance and proper motion from our histogram (Figure 4), we took out stars that did not belong in the cluster.

The generated stellar population models showed us that at 10 million years, most of the stars are on the main sequence. As we moved further down the time sequence, the stars at 100 million years old started to curve towards the right and the magnitudes did not reach the brightness of the younger population. Once we reached the stellar population in the billions of years old, the stars had been reddened and dimmed by almost 8 magnitudes. This goes to show how stars cool down as they age and become redder. We can also see that with the older populations of stars, there are many red giants on the top right portion of the plot. The isochrone population models can help us measure the age of our cluster by fitting the color-magnitude diagram of our cluster to it and seeing what age best fits the data.

All in all, we started with raw images of NGC 2323 from MLO and processed them so that we could get the counts of the stars. The counts were then converted into observed magnitudes. Then we queried two databases to isolate our cluster from other stars in the same line of sight. When we had our separated stars, we measured the counts and found the zeropoint magnitude in order to calculate the observed magnitude. After filtering out stars based on distance and proper motion, we were able to compare stars from NGC 2323 to the model predictions for the best age and color excess.

A study in 2012 by Frolov et al. (2012) used proper motion and photometry to determine the age, distance, and color excess of NGC 2323. They found an age of 125 million years, a distance of 929 pc, and a color excess of 0.213. My results for distance were not too different, but I was unable to get a best fit for age and color excess. I hope to gain more experience calculating the parameters to other celestial objects so that I can have more accurate results in the future.

REFERENCES

Frolov, V. N., Ananjevskaja, Y. K., & Polyakov, E. 2012, Astronomy letters, 38, 74

Gaia Collaboration, Prusti, T., de Bruijne, J. H. J., et al. 2016, A&A, 595, A1, doi: 10.1051/0004-6361/201629512

Henden, A. A., Munari, U., Tomasella, L., et al. 2016, A&A, 588, A89, doi: 10.1051/0004-6361/201527906

Rose, J. A. 2018, PASP, 130, 114501, doi: 10.1088/1538-3873/aad9e9

Starck, J.-L., Murtagh, F., & Bijaoui, A. 2002, Astronomical Image and Data Analysis (Berlin, Germany: Springer)